Vol. 5 №. 4 TRANSACTIONS OF NFsoc Dec. 1995

A MECHANICAL MODEL FOR THE CHIP SIDE DEFORMATION IN ALUMINIUM ALLOY CUTTING①

Xia Wei, Li Yuanyuan, Zhou Zehua
Department of Mechanical Engineering,
South China University of Technology, Guangzhou 510641

ABSTRACT A mechanical model for the chip side deformation in aluminium alloy cutting is developed according to the plasticity theory. The stresses caused by the chip side deformation and their effects on cutting forces of the rectangular groove cutting are analyzed. It is found that the effect of the chip side deformation on the thrust force F_y is much greater than that on the power force F_z. It is therefore believed that in the rectangular groove cutting a steep rise of the thrust force is the main cause to induce the chatter and hence to produce the poor machined surface.

Key words metal cutting mechanical model cutting force chip side deformation

1 INTRODUCTION

It is well known that in metal cutting process the chip deformation will take place not only in length and thickness but also in width. The latter may be defined as the chip side deformation. In orthogonal cutting as is usually studied the chip side deformation can take place freely, having little effect on cutting forces. However in the rectangular groove cutting, as shown in Fig. 1, where *d* is the depth of the machined groove, since the side deformation of the chip BCED in the machined groove is restricted by side-walls of the machined groove, an accompanying stress field is produced, causing a strong friction between two sides of the chip and side-walls of the machined groove when the chip flows, thus having a significant effect on cutting forces. Therefore great attention should be paid to the chip side deformation in the analysis of the rectangular groove cutting.

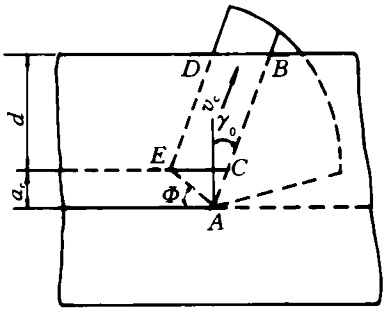

Fig. 1 Rectangular groove cutting

The amount of chip side deformation is influenced by cutting conditions. The detailed analyses concerning the effect of cutting conditions on the chip side deformation and the stress field caused by elastic deformation can be found in refs. [1−3]. What will be primarily concerned with in this paper is the stress field, which is produced when the chip side deformation exceeds the limit of elasticity or yielding occurs, and its effect on cutting forces, since it was observed that for most ductile metals such as aluminium alloy the chip side deformation almost exhibits the plas-

---

① Received Jul. 25, 1995; accepted Sep. 22, 1995

tic deformation[2]. Only the plasticity theory is used in analysis, could the correct results be obtained.

2 MECHANICAL MODEL FOR THE CHIP SIDE DEFORMATION

Fig. 2 shows the stress state of chip in the machined groove when the chip side deformation takes place. In order to determine the stress field caused by the chip side deformation, following four assumptions are introduced.

(a) The chip is an ideal plastic material which does not work-harden, and the deformation is predominantly in plane strain.

(b) Stress components σ_x and σ_y are independent of the coordinate x hence only a function of y.

(c) Friction on the boundary has little effect on the process that material is getting into yielding. Therefore the directions of x and y can be approximately considered as the directions of principal stresses.

(d) The shear stress τ_{xy} is a linear function of x. At the section of $x = 0$ the shear stress τ_{xy} equals zero because of symmetry, and along the boundary of $x = \pm a_w/2$, $\tau_{xy} = \mu\sigma_x$, where μ is the frictional coefficient between the chip and the side-walls of machined groove.

For the case of plane strain, we have the following equations of equilibrium

$$\begin{cases} \dfrac{\partial\sigma_x}{\partial x} + \dfrac{\partial\tau_{xy}}{\partial y} = 0 \\ \dfrac{\partial\tau_{xy}}{\partial x} + \dfrac{\partial\sigma_y}{\partial y} = 0 \end{cases} \tag{1}$$

From Fig. 2 the boundary conditions may be written by

$$\begin{cases} [\sigma_y]_{y=a_0} = 0, & [\tau_{xy}]_{y=a_0} = 0 \\ [\tau_{xy}]_{x=\pm a_w/2} = \mu\sigma_x, & [\tau_{xy}]_{x=0} = 0 \end{cases} \tag{2}$$

When yielding occurs in the chip, the Mises criterion for the conditions of plane strain

$$(\sigma_1 - \sigma_3)^2 = 4k^2 \tag{3}$$

can be employed, where k is the yield shear stress of material. According to assumption (c) equation (3) becomes

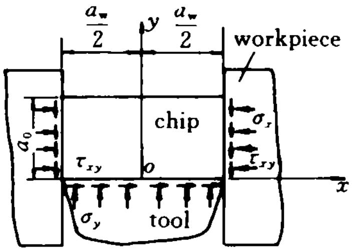

Fig. 2 Stress state of the chip in groove

$$\sigma_x - \sigma_y = 2k \tag{4}$$

On the basis of assumption (d), together with the boundary conditions (2) we obtain

$$\tau_{xy} = 2\mu\sigma_x x/a_w \tag{5}$$

According to assumption (b), upon substitution of equations (4) and (5), the second equation of (1) becomes

$$\frac{d\sigma_x}{dy} + \frac{2\mu\sigma_x}{a_w} = 0 \tag{6}$$

Direct integration of the above equation gives

$$\sigma_x = c\exp(-2\mu y/a_w) \tag{7}$$

where c is a constant of integration, which can be evaluated by applying the boundary conditions (2) and equation (4). Expressions for σ_y and τ_{xy} follow from equations (4) and (5). Finally the stress fields are found to be

$$\begin{cases} \sigma_x = 2k\exp[2\mu(a_0 - y)/a_w] \\ \sigma_y = 2k\{\exp[2\mu(a_0 - y)/a_w] - 1\} \\ \tau_{xy} = 4\mu kx\exp[2\mu(a_0 - y)/a_w]/a_w \end{cases} \tag{8}$$

3 FORCES CAUSED BY THE CHIP SIDE DEFORMATION

Cutting forces caused by the chip side deformation can now be calculated according to the stress field (8). In the rectangular groove cutting since the chip side deformation is restricted, some accompanying forces are exerted on the chip. As shown in Fig. 3, N_t represents the normal force acting on the bottom of the chip; N_w the normal force acting on the sides of the chip; F_t the frictional force between the tool face and the chip; F_w the frictional force between the side-walls of the machined groove and the chip. Assume that μ_t is the frictional coefficient between the tool face

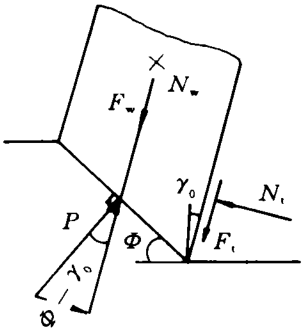

Fig. 3 Forces caused by the chip side deformation

and the chip, and μ_w between the side-walls of the machined groove and the chip, then we have

$$F_t = \mu_t N_t \tag{9}$$

$$F_w = 2\mu_w N_w \tag{10}$$

It is obvious that in cutting process an additional force is needed to overcome these two frictional forces for the chip to flow. Assuming that this additional force P is normally exerted on the chip at the shear plane. Referring to Fig. 3, the component of P in the direction of chip flow, $P\cos(\Phi - \gamma_0)$, which is the force needed to overcome the friction, should be balanced by frictional forces F_t and F_w, that is

$$P\cos(\Phi - \gamma_0) = F_t + F_w \tag{11}$$

While another component of P, $P\sin(\Phi - \gamma_0)$, acts on the tool face through the chip, increasing the compressive force on the tool face. In the meantime, the compressive stress produced by the chip side deformation σ_y has also an effect on the tool face. Assume that N_{ts} is the compressive force acting on the tool face owing to σ_y, then the following equation should be satisfied

$$N_t = N_{ts} + P\sin(\Phi - \gamma_0) \tag{12}$$

Substituting equations (9) and (10) into (11), together with (12), we obtain

$$P = \frac{\mu_t N_{ts} + 2\mu_w N_w}{\cos(\Phi - \gamma_0)[1 - \mu_t \tan(\Phi - \gamma_0)]} \tag{13}$$

In which N_{ts} and N_w can be calculated by using equation (8) above, that is

$$N_{ts} = \frac{d}{\cos\gamma_0}\int_{-a_w/2}^{a_w/2}[\sigma_y]_{y=0}\mathrm{d}x \tag{14}$$

$$N_w = \frac{d}{\cos\gamma_0}\int_0^{a_0}[\sigma_x]_{x=a_w/2}\mathrm{d}y \tag{15}$$

where

$$a_0 = \frac{\cos(\Phi - \gamma_0)}{\sin\Phi}a_c \tag{16}$$

Replacing μ in equation (8) with μ_w and then substituting equation (8) into (14) and (15) respectively gives

$$\begin{cases} N_{ts} = \dfrac{2ka_w d}{\cos\gamma_0}\{\exp[2\mu_w\rho\cos(\Phi - \gamma_0)/ \\ \qquad \sin\Phi] - 1\} \\ N_w = N_{ts}/(2\mu_w) \end{cases} \tag{17}$$

where $\rho = a_c/a_w$.

The additional force P can now be found out by using equations (13) and (17). Let $F_z^{(2)}$ and $F_y^{(2)}$ represent respectively the power force and the thrust force caused by the chip side deformation, from Fig. 3 we can thus obtain

$$\begin{cases} F_z^{(2)} = P\sin\Phi \\ F_y^{(2)} = P\cos\Phi \end{cases} \tag{18}$$

Therefore the total cutting forces of the rectangular groove cutting, when the effect of chip side deformation on cutting forces is taken into account, can be expressed as

$$\begin{cases} F_z = F_z^{(0)} + F_z^{(1)} + F_z^{(2)} \\ F_y = F_y^{(0)} + F_y^{(1)} + F_y^{(2)} \end{cases} \tag{19}$$

where $F_z^{(0)}$, $F_y^{(0)}$ are respectively the power force and thrust force produced by the tool major cutting edge, and $F_z^{(1)}$, $F_y^{(1)}$ by the tool minor cutting edges. As has been analyzed in refs. [2, 3], they can be written by

$$F_z^{(0)} = \frac{\tau_s a_c a_w \cos(\beta - \gamma_0)}{\sin\Phi\cos(\Phi + \beta - \gamma_0)}$$

$$F_y^{(0)} = \frac{\tau_s a_c a_w \sin(\beta - \gamma_0)}{\sin\Phi\cos(\Phi + \beta - \gamma_0)}$$

$$F_z^{(1)} = (K - 1)F_z^{(0)}$$

$$F_y^{(1)} = (K - 1)F_y^{(0)}$$

$$K = 1 + \rho(\cot\Phi + \tan\gamma_0) \times$$

$$[\sin\Phi\sqrt{\frac{\cos^2\gamma_0 + \tan^2\varphi}{\cos^2\gamma_0 + \tan^2\varphi\cos^2(\Phi - \gamma_0)}} +$$

$$\frac{\sin\varphi\sin 2\Phi\sqrt{\cos^2\gamma_0 + \tan^2\varphi}}{2\cos\gamma_0} - \tan\varphi]$$

From equation (18) it can be seen that $F_y^{(2)}$ is greater than $F_z^{(2)}$ since the shear angle Φ

is usually smaller than 45°. In other words the effect of the chip side deformation on the thrust force F_y is more remarkable than that on the power force F_z. The reason is the fact that the orientation of the frictional forces F_t and F_w is governed by the direction of chip flow, leading to a greater component in the direction of F_y, which is more notable especially with a smaller tool rake angle or/and shear angle. For this reason it can be predicted that in such cuttings as the rectangular groove cutting and the cut-off cutting, etc., the thrust force F_y will increase more rapidly than the power force F_z does. And it is also believed that a steep rise of the thrust force is the main cause to induce the chatter and hence to produce the poor machined surface.

4 COMPARISION WITH EXPERIMENT

Experiments on the cutting forces of the rectangular groove cutting were run on a vertical milling machine. The cutting tool (H. S. S.) was fitted to the stationary taper hole of the spindle by a special fixture. The workpiece (LY12 Al-alloy) was clamped on a piezoelectrical dynamometer (KISTLER) which was in turn secured to the table. All the cutting tests were performed by feeding the workpiece past the stationary tool at a speed of 0.015m/s. The data of cutting forces were sampled and processed by use of a computer aided test system.

The theoretical values of the cutting forces, which are calculated according to equation (19), are compared with experimental data in Figs. 4~7, theoretical curves being in solid lines. It is suggested[4], while calculating with equation (19), that following data could be used for an aluminium alloy workpiece, i.e. $\mu_t = 0.17$, $\mu_w = 0.22$ and $k = 158$MPa, and the remainders are referred to ref. [2].

Fig. 4 and Fig. 5 show the variation of the two force components, F_z and F_y, with the undeformed chip thickness a_c, and Fig. 6 and Fig. 7 with the depth of machined groove d. It

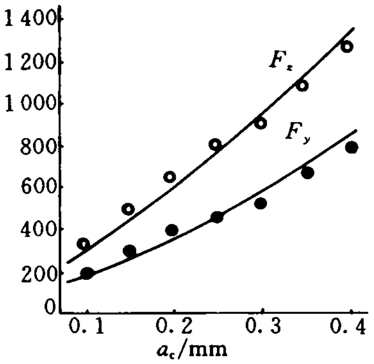

Fig. 4 Variation of cutting forces with undeformed chip thickness
$\gamma_0 = 10°$; $v = 0.015$m/s; $a_w = 4$mm; $d = 2$mm

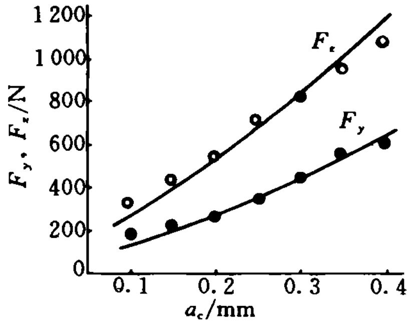

Fig. 5 Variation of cutting forces with undeformed chip thickness
$\gamma_0 = 20°$; remainders are the same as in Fig. 4

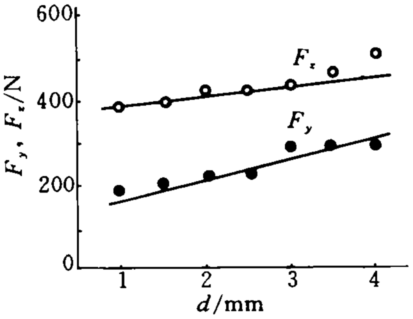

Fig. 6 Variation of cutting forces with depth of the machined groove
$\gamma_0 = 10°$; $v = 0.015$m/s; $a_w = 4$mm; $a_c = 0.15$mm

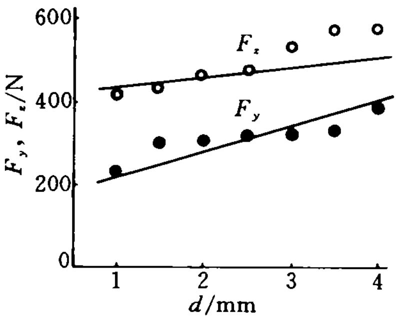

Fig. 7 Variation of cutting forces with depth of the machined groove

$\gamma_0 = 20°$; remainders are the same as in Fig. 6

is seen from the figures that the theoretical values are better consistent with experimental results. Cutting forces increase in proportion with increase of the depth of machined groove. In addition it can be clearly seen, from Fig. 6 and Fig. 7, that as the depth of machined groove d increases both theoretical and experimental values of F_y increase more rapidly than those of F_z. This variation is more remarkable especially with the smaller tool rake angle hence the smaller shear angle. Because d only affects $F_z^{(2)}$ and $F_y^{(2)}$, the fact that F_y increases more rapidly than F_z shows that $F_y^{(2)}$ is greater than $F_z^{(2)}$. Thus equation (18) is further verified experimentally here.

5 CONCLUSIONS

(1) In such deformation-restricted cuttings as the rectangular groove cutting and the cut-off cutting, etc., the chip side deformation has a great effect on the cutting forces. Further research work is therefore necessary.

(2) For most of the ductile metals such as aluminium alloy the chip side deformation almost exhibits the plastic deformation. Only the plasticity theory is used in analysis, could the correct results be obtained.

(3) The chip side deformation has a much greater effect on the thrust force than on the power force. It is therefore believed that in rectangular groove cutting a steep rise of the thrust force is the main cause to induce the chatter and hence to produce the poor machined surface.

REFERENCES

1 Лоладзе Т Н. Стружкообразование при резании металлов. МАШГИЗ, 1952.

2 Xia Wei. PhD Thesis (in Chinese), South China University of Technology, Guangzhou, China, 1988.

3 Xia Wei, Zhou Zehua. Journal of South China University of Technology (in Chinese), 1987, 15(4): 18.

4 Chinese Agriculture Mechanization Science Institute. Practical Machine Design Manual (in Chinese). Beijing: Chinese Agriculture Machine Press, 1985.

5 Usui E, Shirakashi T. Mechanics of Metal Machining. Beijing: National Defence Industry Press, 1984.

6 Slater R A C. Engineering Plasticity Theory and Application to Metal Forming Processes. Macmillan Press Ltd, 1977.

7 Xu Bingye, Chen Sencan. A Course in Plasticity Theory (in Chinese). Beijing: Tsinghua University Press, 1986.

(Edited by Peng Chaoqun)